

Design and Fabrication of a Compact UWB BPF with Notch-Band and Wide Stopband Using Dual MMRs and DGS

Hassiba Louazene^{1, 2, *}, Mouloud Challal², and M'hamed Boulakroune³

Abstract—This paper presents a new design of a compact microstrip ultra-wideband (UWB) single notch-band bandpass filter (BPF) along with its equivalent circuit model. The basic structure of the proposed filter consists of dual symmetrical multiple-mode resonator (MMR), four stub-loaded stepped impedance resonators (SLSIRs), two defected ground structure (DGS) units, and a coupled folded arm resonator (CFAR) with feeding line. The presented filter is tested using R&S® ZNB20 vector network analyzer (VNA) to validate the simulated results. A good agreement between the measured and simulated (EM and circuit model) results is achieved.

1. INTRODUCTION

The unlicensed use of ultra-wideband (UWB) frequency spectrum for short-range communications (3.1 to 10.6 GHz) was approved by the Federal Communications Commission (FCC) in 2002 [1]. UWB bandpass filters (BPFs) with small size and having good frequency characteristics like low insertion loss in the passband and good selectivity are essential key components of the modern day communication systems.

Lately, UWB filters have been developed using multiple-mode resonators (MMRs) [2–8]. Different filter topologies based on MMR configuration along with stepped impedance [2], rectangle-shaped defected ground structure (DGS) unit and two symmetrical MMRs linked to quarter-wavelength parallel coupled lines [5], broadside-coupled microstrip, open loop resonator and DGS units [8] were investigated. Nevertheless, erroneous resonant passbands affect the majority of these UWB filters. As a result, several methods for improving the upper stopband of UWB filters have been described and studied in the literature, including spur-line structures [9], stepped impedance stub loaded resonators [10], stepped impedance resonator [11], cascading E-shape microstrip structures [12], and cascading several open-circuited transmission line sections [13]. On the other hand, these filter types can interfere with undesired narrow-band radio frequencies like WLAN and some satellite communication systems. UWB-BPFs with one or more notched bands are needed to eliminate these conflicting signals. To overcome such interference, many design suggestions have been presented in [14–16]. For example, a quarter-wavelength meander slot-line structure created a notch at 5.8 GHz [17], and a narrow head stub and two asymmetric stubs were connected to form a notched band from 5.65–5.8 GHz [18]. In [19], a loaded stub capacitor created a notched band ranging from 3.7 to 7.7 GHz.

In this paper, a novel compact UWB-BPF with single notch-band and wide upper stopband is investigated. The proposed filter consists of two symmetrical MMRs, four stub-loaded stepped impedance resonators (SLSIRs), and two rectangular DGS units. To isolate interferences from wireless

Received 20 November 2022, Accepted 14 February 2023, Scheduled 2 March 2023

* Corresponding author: Hassiba Louazene (louazene.hassiba@univ-ouargla.dz).

¹ Department of Electronics and Telecommunications, Faculty of New Technologies of Information and Telecommunication, Kasdi MERBAH University of Ouargla, Ouargla, Algeria. ² Signals and Systems Laboratory, Institute of Electrical and Electronic Engineering, University M'hamed BOUGARA of Boumerdes, Boumerdes, Algeria. ³ Department of Electrical and Automatic, National Polytechnic School of Constantine, Constantine, Algeria.

local area network (WLAN) band, a coupled folded arm resonator (CFAR) is inserted with a feeding line. To understand the behavior of the design, an equivalent circuit model for the proposed filter is developed. The design process is performed by full wave electromagnetic (EM) IE3D software. Details of the filter design, fabrication, and measurement are presented and discussed.

2. FILTER DESIGN

Figure 1 shows the configuration of the proposed UWB-BPF, fed by a 50 ohm microstrip line, with a notch band. The filter consists of two symmetrical MMRs in a parallel-connected configuration with four SLSIRs and two rectangular DGS units. To reject a 6.2 GHz narrow band, a CFAR is added with a feeding line. The proposed notched-band UWB-BPF dimensions are indicated in Fig. 1, and their optimized values are reported in Table 1.

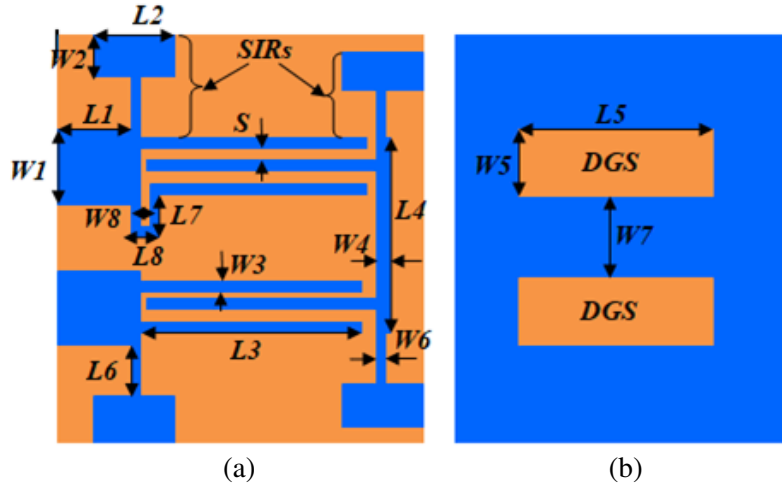


Figure 1. Proposed UWB-BPF with a notched band. (a) Top view and, (b) bottom view.

Table 1. Optimized parameters of the proposed single notch band UWB-BPF.

Parameter	L1	L2	L3	L4	L5	L6	L7	L8	/
Dimension (mm)	5.59	4.44	5.52	12.305	6	6.64	2	0.9	/
Parameter	W1	W2	W3	W4	W5	W6	W7	W8	S
Dimension (mm)	3.15	2.6	0.3	0.61	3	0.31	8.695	0.3	0.3

Figure 2 shows different design steps of the proposed UWB-BPF. Filter A structure consists of a single MMR connected to two SLSIRs positioned above the substrate and a DGS unit, which is realized by etching rectangular defects on the ground plane of the substrate. The next filter, Filter B, is obtained by combining two filters of type A in order to enhance the upper stopband response. The third and last filter, Filter C, is simply Filter B structure with a CFAR inserted with a feeding line. The simulated insertion loss characteristics for the three developed prototypes of the proposed filters are shown in Fig. 3. According to the graphs, the reference filter, Filter A, has a narrow upper stopband, from 12 GHz to 13 GHz, with attenuation loss less than 15 dB and an ultra-bandwidth of 112.32%, extending from 3.2 GHz to 11.4 GHz. Filter B structure has a broad upper stopband from 12 GHz to 25 GHz with attenuation loss superior to 15 dB and occupies a 98.92% ultra-bandwidth, from 3.3 GHz to 9.75 GHz, with low insertion loss of 0.8 dB. The structure of Filter C has an ultra-bandwidth of 98.92% with attenuation loss higher than 15 dB and low insertion loss of 0.8 dB.

Parametric studies are done to comprehend how some crucial filter parameters affect the notched properties. Fig. 4(a) depicts the insertion loss graph after changing the length of the coupled arm

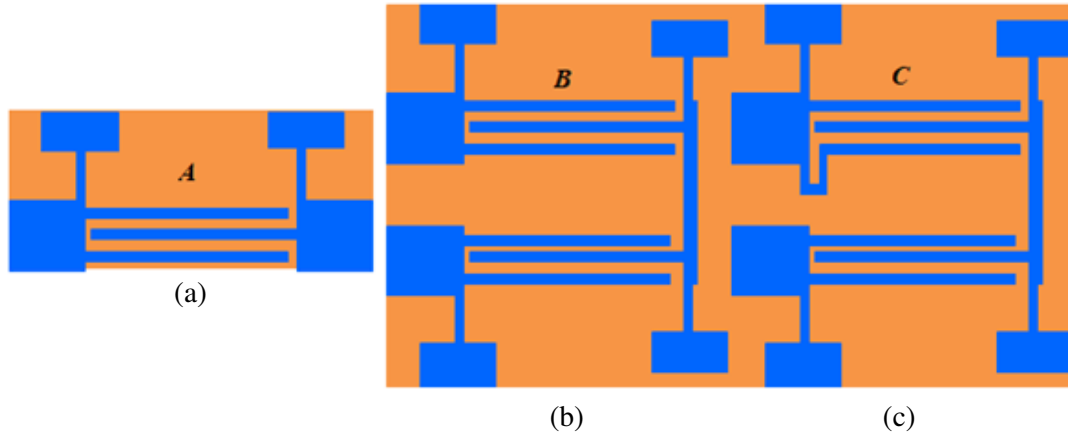


Figure 2. Design steps of the proposed UWB-BPF. (a) Filter A, (b) Filter B and, (c) Filter C.

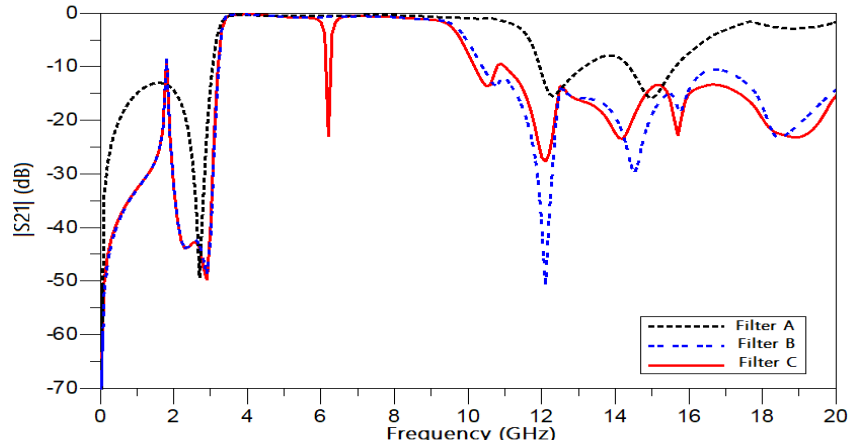


Figure 3. Simulated S_{21} parameters of different filter configurations.

($L7$). The 3dB notched bandwidth increases from 0.15 GHz (for $L = 1.40$ mm), 0.35 (for $L = 2$ mm) to 0.45 GHz (for $L = 2.59$ mm), and its center frequency moves to a lower frequency range. Fig. 4(b) illustrates the impact of the folded arm resonator gap ($W8$). The graph shows that when $W8$ rises, the notch frequency decreases with some bandwidth reductions. Fig. 4(c) shows the effect of varying the length $L4$. It can be observed that when $L4$ rises, the upper stopband attenuation rises as well with a fixed notch center frequency.

Figure 5 illustrates the surface current distribution of the notchband filter structure at 6.2 GHz (i.e., notch-band frequency). From Fig. 5, it can be seen that the CFAR has a very high current concentration at a frequency of 6.2 GHz. This indicates that the resonator is tightly connected to the fundamental UWB filter at its notch-band frequency (6.2 GHz). Furthermore, Fig. 5 tells us that the resonator dimensions cause the creation of transmission zeros (TZs) in the UWB spectrum.

In order to analyze the behavior of the proposed filter, an equivalent circuit model is developed as shown in Fig. 6(a). The parameters of the MMR curve, as a function of the inductances ($L2$, $L3$, and $L4$) and capacitance ($C2$), determine the passband width of the UWB filter [20]. In addition, the parallel arrangement of $L1$ and $C1$, which are connected via $C0$, depicts the microstrip line that joins the two MMRs. Through $C5$ and $C6$, this microstrip line is capacitively linked to the DGS in the ground plane, whereas the circuit of $L5$, $C3$, and $C4$ represents the DGS unit. $L6$ and $C8$ are arranged in parallel to represent the coupled folded arm and are connected in series with $C7$.

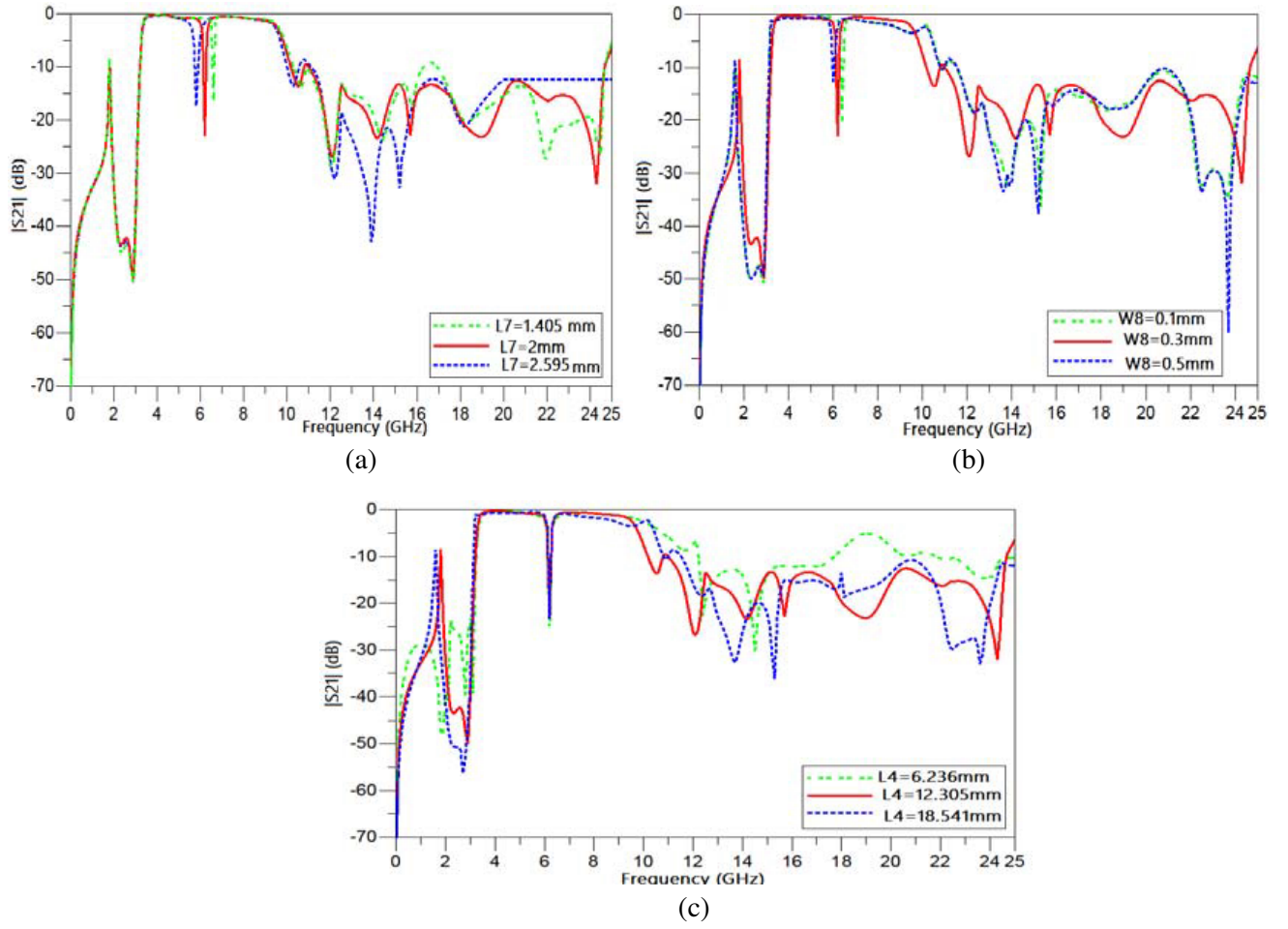


Figure 4. Simulated S_{21} for different values of (a) $L7$, (b) $W8$ and, (c) $L4$.

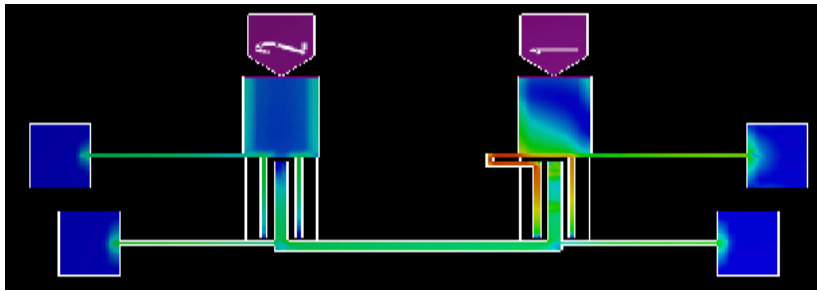


Figure 5. Current distribution at 6.2 GHz.

The following equation relates the notch location to the lumped parameters:

$$f(6.2 \text{ GHz}) = \frac{1}{2\pi\sqrt{(L6C8 + L6C7)}} \quad (1)$$

To get the appropriate response, the lumped components are adjusted and optimized using advanced design system (ADS) software. These are the optimal lumped parameters: $L1 = 2.9 \text{ nH}$, $L2 = 1.71 \text{ nH}$, $L3 = 1.32 \text{ nH}$, $L4 = 6.5 \text{ nH}$, $L5 = 1.482 \text{ nH}$, $L6 = 0.95 \text{ nH}$, and $C0 = 0.0044 \text{ pF}$, $C1 = 1.3 \text{ pF}$, $C2 = 4.2 \text{ pF}$, $C3 = 0.385 \text{ pF}$, $C4 = 0.303 \text{ pF}$, $C5 = 0.132 \text{ pF}$, $C6 = 0.132 \text{ pF}$, $C7 = 0.328 \text{ pF}$,

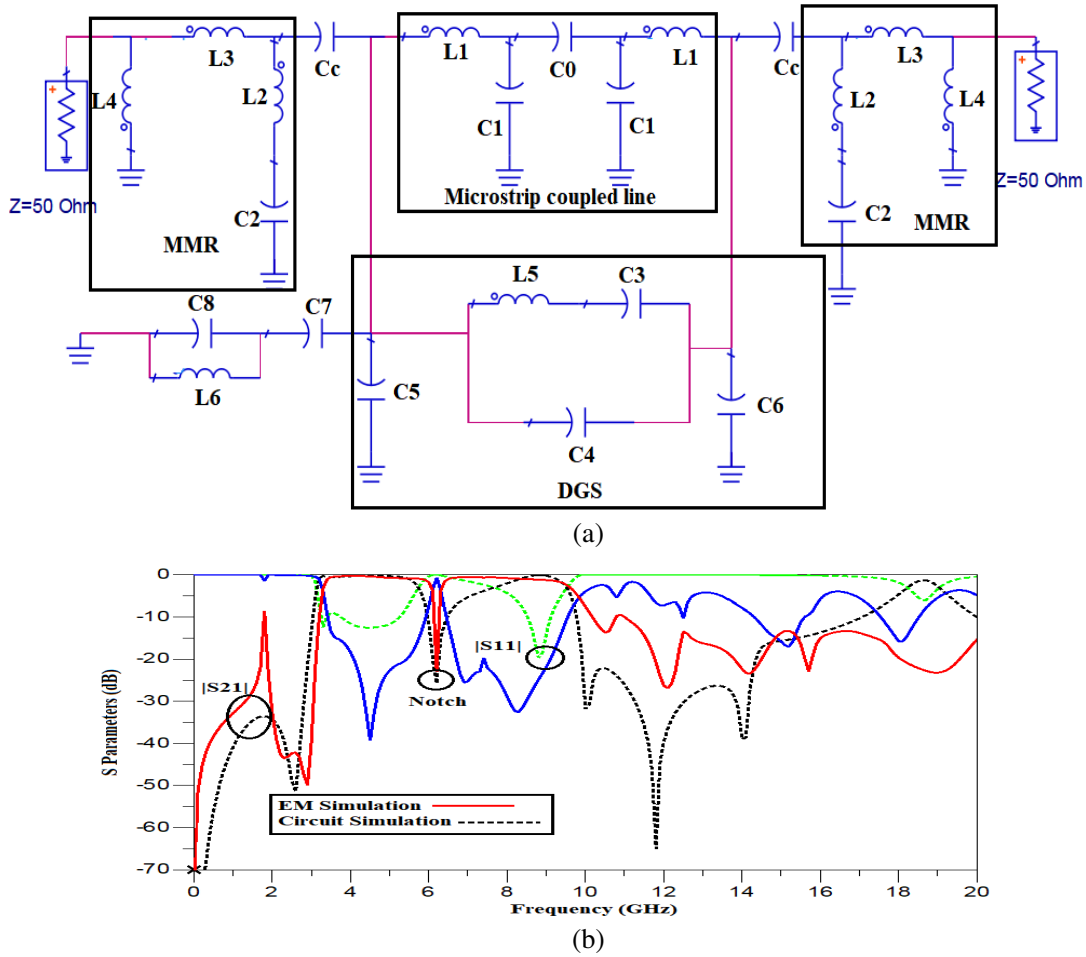


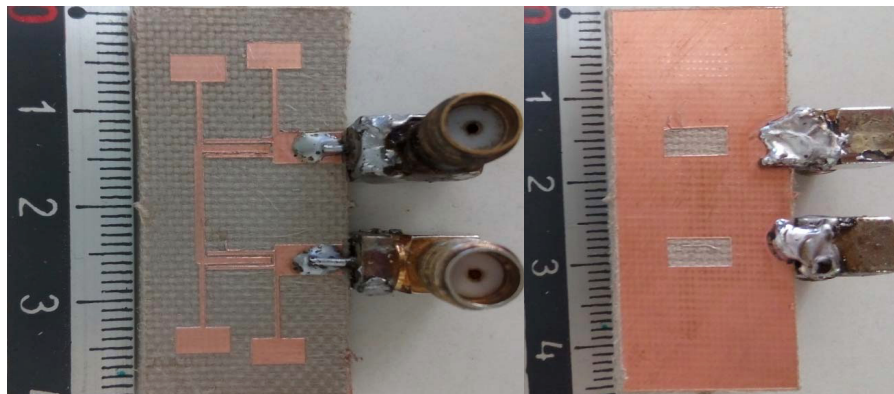
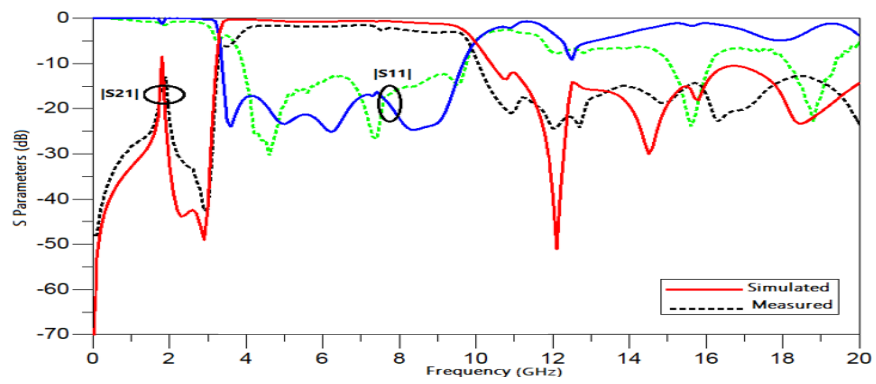
Figure 6. Equivalent circuit model for the proposed structure. (a) An electrical circuit consisting of an inductor (L), and a capacitor (C), (b) S -parameters comparison between equivalent circuit and EM simulations.

$C_8 = 0.374\text{ pF}$, $C_c = 0.61\text{ pF}$. Fig. 6(b) depicts the comparison of S -parameters between equivalent circuit and EM simulations.

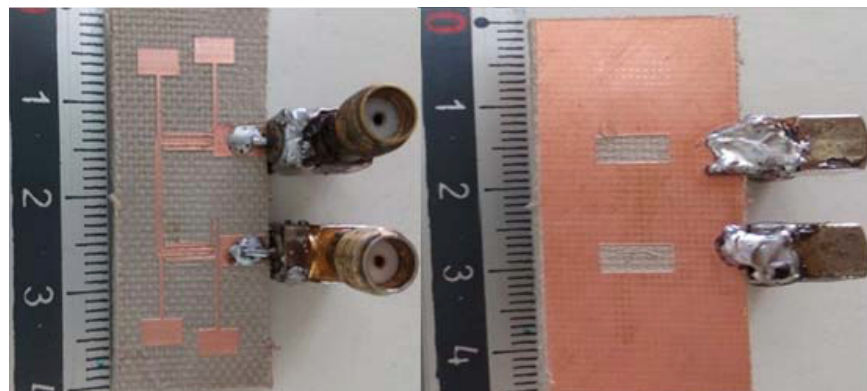
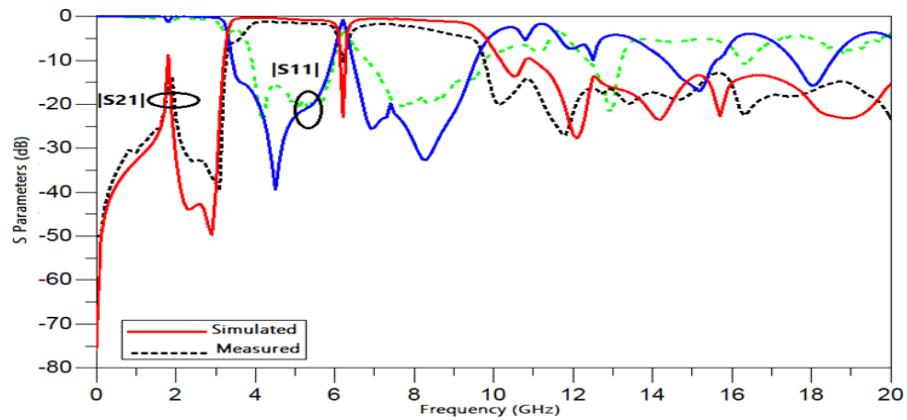
3. EXPERIMENTAL VERIFICATION

The proposed filters, without and with a narrow notch band, are fabricated using a PCB prototype machine as shown in Fig. 7. The prototype testing is performed by using a Roche & Schwarz ZNB20 vector network analyzer (VNA) operating from 10 kHz to 20 GHz. Fig. 7(a) displays the simulated and measured S parameters of the proposed filter without a notch band. The observed bandwidth ranges from 3.8 to 9.5 GHz with an insertion loss of 1.8 dB and a return loss of more than 3 dB. The stopband has an attenuation loss greater than 13 dB which is wide up to 2 GHz.

From Fig. 7(b), it is evident that the response of the proposed filter, with a single notch band, exhibits a passband bandwidth from 3.8 to 9 GHz which corresponds to the UWB spectrum designated by the FCC. The attenuation loss of the notch, located at 6.2 GHz, is higher than 11 dB. The insertion loss is less than 2 dB, and the return loss is more than 15.75 dB over the passband except for the notch. The stopband has an attenuation loss greater than 13 dB which is extended up to 2 GHz. Fig. 7(c) shows group delay comparison between simulated and measured results. The group delay is flat and modest, spanning between 0.2 and 0.5 ns.



(a)



Top View

Bottom View

(b)

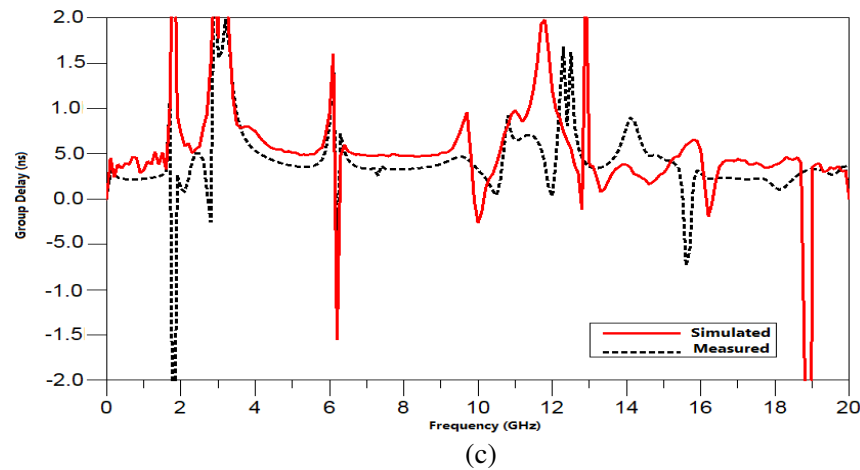


Figure 7. *S*-parameters comparison between measured and simulated results, (a) UWB-BPF without a notch band, (b) UWB-BPF with a narrow notch band and, (c) comparison of group delay between measured and simulated data.

Table 2 compares the performance of the proposed UWB-BPF with notched band to other UWB filters designs reported in the literature. It is noticeable from Table 2 that the presented design is distinct from the others, and the performances are comparable to the other designs. The proposed filter is superior in terms of wide stopband response and relatively quick roll-off rate and small in size.

Table 2. Comparison between current design and previous related works.

Ref	Used material ϵ_r/h (mm)	Notches (GHz)/ attenuation (dB)	Notch technique	Stopband (GHz)/ Attenuation (dB)	roll-off rate (dB/GHz)	Size ($\lambda_g \times \lambda_g$)
[21]	FR4 (4.4/1.6)	5.8/60	SIR	14/20	11.88	0.47×0.26
[22]	FR4 (4.6/0.8)	5.1/45	$\lambda/4$ short-circuit SIS	12/10	17	0.28×0.09
[23]	FR4 (4.4/1.6)	5.2/20	DMS	14/12	21.25	0.83×0.55
[24]	Rogers Ro5880 (2.2/0.5)	7/20	L-shaped resonator	18/10	23.8	0.4×0.26
[25]	Rogers 5880 (2.2/0.5)	5.85/19	stepped slot	18/10	49	0.78×0.19
[26]	FR4 (4.3/1.62)	5.8/22	DGS units	14/12	-	1.12×0.16
[27]	Rogers RO-4350 (3.66/0.76)	5.1–8.3/19–15	inverted E and T shaped SR	10.6/10	-	0.06×0.02
[28]	Rogers RO4350 (3.66/0.5)	5.8/30	CRR	14/20	24.28	0.81×0.4
This work	FR4 (4.3/1.62)	6.2/11	CFAR	20/13	17	0.69×0.32

4. CONCLUSION

In this article, a new structure of a single notch band UWB-BPF has been presented. The filter has been designed based on two symmetrical MMRs, four SLSIRs, two DGS units, and a CFAR with feeding line. The proposed filter has been successfully simulated, fabricated, and tested. The measurement results have shown that the filter response had a passband range from 3.8 and 9 GHz. The insertion loss in the entire passband was less than 2 dB, and the return loss was around 13 dB on average extended up to 20 GHz. The notch band with an attenuation of around 11 dB at 6.2 GHz had a sharp attenuation. The group delay was between 0.2 and 0.5 ns. An acceptable agreement has been achieved between the simulated (EM and circuit model) and measured results. Because of its small size, the proposed prototype is simple to incorporate into current communication networks.

ACKNOWLEDGMENT

The authors thank Dr. F. Mouhouche, University M'Hamed BOUGARA of Boumerdes, for the provided help during the fabrication and measurement process.

REFERENCES

1. Federal Communications Commission, "Revision of Part 15 of the Commission's rules regarding ultra-wideband transmission systems," Tech. Rep., ET-Docket 98-153, FCC02-48, Apr. 2002.
2. Zhu, L., Sh. Sun, and W. Menzel, "Ultra-wideband (UWB) bandpass filters using multiple-mode resonator," *IEEE Microwave and Wireless Components Letters*, Vol. 15, No. 11, 796–798, Nov. 2005.
3. Chakraborty, P., P. P. Shome, A. Deb, A. Neogi, and J. R. Panda, "Compact configuration of open ended stub loaded multi-mode resonator based UWB bandpass filter with high selectivity," *2021 8th International Conference on Signal Processing and Integrated Networks (SPIN)*, 59–63, 2021, doi: 10.1109/SPIN52536.2021.9565956.
4. Weng, M. H., C.-T. Liauh, H.-W. Wu, and S. R. Vargas, "An ultra-wideband bandpass filter with an embedded open-circuited stub structure to improve in-band performance," *IEEE Microwave and Wireless Components Letters*, Vol. 19, No. 3, 146–148, Mar. 2009, doi: 10.1109/LMWC.2009.2013733.
5. Louazene, H., M. Challal, and M. Boulakroune, "Compact ultra-wide band bandpass filter design employing multiple-mode resonator and defected ground structure," *Procedia Computer Science*, Vol. 73, 376–383, Dec. 2015, doi: 10.1016/j.procs.2015.12.006.
6. Louazene, H., M. Boulakroune, and M. Challal, "UWB microstrip bandpass filter using multiple-mode resonator and rectangular-shaped DGS," *International Conference on Telecommunication and Applications (ICTA-14)*, Béjaia, Algeria, Apr. 23–24, 2014.
7. Boulakroune, M., M. Challal, H. Louazene, and S. Fentiz, "Design and synthesis of two tunable bandpass filters based on varactors and defected ground structure," *International Journal of Electrical, Computer, Electronics and Communication Engineering*, Vol. 9, No. 3, 271–275, 2015, doi: 10.5281/zenodo.1099706.
8. Louazene, H., M. Boulakroune, and M. Challal, "The broadside-coupled microstrip structure using open loop resonator DGS," *The 2014 International Symposium on Networks, Computers and Communications*, 1–4, 2014, doi: 10.1109/SNCC.2014.6866532.
9. Ghazali, A. N. and A. Singh, "Broadside coupled UWB filter with dual notched band and extended upper stopband," *2014 International Conference on Devices, Circuits and Communications (ICDCCom)*, 1–5, 2014, doi: 10.1109/ICDCCom.2014.7024701.
10. Chu, Q.-X. and X.-K. Tian, "Design of UWB bandpass filter using stepped-impedance stub-loaded resonator," *IEEE Microwave and Wireless Components Letters*, Vol. 20, No. 9, 501–503, Sept. 2010, doi: 10.1109/LMWC.2010.2053024.
11. Khalid, S. and S. Q. Ali, "Design of highly selective ultra-wideband (UWB) bandpass filter using step impedance resonator and parallel coupled lines," *2015 Symposium on Recent Advances in Electrical Engineering (RAEE)*, 1–4, 2015, doi: 10.1109/RAEE.2015.7352760.

12. Hammed, R. T. and D. Mirshekar-Syahkal, "High-order UWB bandpass filter using cascaded E-shape microstrip structure," *2011 IEEE MTT-S International Microwave Symposium*, 1–4, 2011, doi: 10.1109/MWSYM.2011.5972811.
13. Zhang, T., F. Xiao, X. Tang, and L. Guo, "A multi-mode resonator-based UWB bandpass filter with wide stopband," *International Journal of Microwave and Wireless Technologies*, Vol. 8, No. 7, 1031–1035, Nov. 2016, doi: 10.1017/S1759078715001026.
14. Louazene, H., M. Challal, and M. Boulakroune, "Compact UWB BPF with notch-band using SIR and DGS," *Int. J. High Performance Computing and Networking*, Vol. 11, No. 2, 167–172, 2018, doi: 10.1504/IJHPCN.2018.089889.
15. Wu, Z., Y. Shim, and M. Rais-Zadeh, "Miniaturized UWB filters integrated with tunable notch filters using a silicon-based integrated passive device technology," *IEEE Transactions on Microwave Theory and Techniques*, Vol. 60, No. 3, 518–527, Mar. 2012, doi: 10.1109/TMTT.2011.2178428.
16. Louazene, H., M. Challal, and M. Boulakroune, "Band-notched ultra-wideband bandpass filter design using multiple-mode resonator and stepped impedance stub loaded," *2017 5th International Conference on Electrical Engineering — Boumerdes (ICEE-B)*, 1–5, 2017, doi: 10.1109/ICEE-B.2017.8192151.
17. Luo, X., J.-G. Ma, K. Ma, and K. S. Yeo, "Compact UWB bandpass filter with ultra narrow notched band," *IEEE Microwave and Wireless Components Letters*, Vol. 20, No. 3, 145–147, Mar. 2010, doi: 10.1109/LMWC.2010.2040212.
18. Shavakand, M. Y. and J. A. Shokouh, "Compact UWB filter with narrow notched band based on grounded circular patch resonator," *Int. J. Ultra Wideband Communications and Systems*, Vol. 4, No. 1, 2019, doi: 10.1504/IJUWBCS.2019.101173.
19. Zhou, J. Ch., P. Guo, and W. Wu, "Compact UWB BPF with a tunable notched band based on triple-mode HMSIW resonator," *I.J. Wireless and Microwave Technologies*, Vol. 1, 1–12, 2016, doi: 10.5815/ijwmt.2016.01.01.
20. Ghazali, A. N. and S. Pal, "UWB-BPF with application based triple notches and suppressed stopband," *Progress In Electromagnetics Research C*, Vol. 39, 149–163, 2013.
21. Sen, S. and T. Moyra, "Modeling of a compact ultra-wideband bandpass filter with a single notch using DGS and DMS technology," *Waves in Random and Complex Media*, 2021, doi: 10.1080/17455030.2021.1987585.
22. Liu, L.-Q., H.-S. Lai, H.-M. Hu, J.-J. Chen, M.-H. Weng, and R.-Y. Yang, "A simple method to design a UWB filter with a notched band using short-circuit step impedance stubs," *Electronics*, Vol. 11, 1124, 2022, <https://doi.org/10.3390/electronics11071124>.
23. Azizi, S., M. El Gharbi, S. Ahyoud, and A. Asselman, "Design and analysis of compact microstrip UWB band pass filter with a notched band using defected microstrip structure," *Procedia Manufacturing*, Vol. 32, 669–674, 2019, doi: 10.1016/j.promfg.2019.02.269.
24. Huang, L., M. Li, P.-J. Zhang, K. Duan, and Y. Song, "A novel miniaturized UWB bandpass filter basing on E-shaped defected microstrip structure," *Progress In Electromagnetics Research Letters*, Vol. 93, 49–57, 2020.
25. Zhang, T., F. Xiao, J. Bao, and X. Tang, "A compact UWB bandpass filter with a notched band using a multistubs loaded resonator," *International Journal of RF and Microwave Computer-Aided Engineering*, Vol. 27, No. 1, 2017, doi: 10.1002/mmce.21054.
26. Challal, M., "Design and fabrication of a compact UWB filter with WLAN stopband rejection characteristic," *The 4th International Conference on Recent Advances in Electrical Systems — ICRAES'19*, Hammamet, Tunisia, Dec. 23–25, 2019, ISBN: 978-9938-9937-2-1.
27. Basit, A., M. I. Khattak, and M. Alhasan, "Design and analysis of a microstrip planar UWB bandpass filter with triple notch bands for WiMAX, WLAN, and X-band satellite communication systems," *Progress In Electromagnetics Research M*, Vol. 93, 155–164, 2020.
28. El Bakalia, H. E., H. Elftouha, A. Farkhsia, and A. Zakriti, "A compact UWB bandpass filter with WLAN band rejection using hybrid technique," *Procedia Manufacturing*, Vol. 46, 922–926, 2020, doi: 10.1016/j.promfg.2020.05.009.